Seasonal Synchronization in a Chaotic Ocean–Atmosphere Model

RAFFAELE FERRARI*

Woods Hole Oceanographic Institution, Woods Hole, Massachusetts

PAOLA CESSI

Scripps Institution of Oceanography, University of California, San Diego, La Jolla, California

(Manuscript received 5 December 2001, in final form 23 August 2002)

ABSTRACT

The signatures of feedback between the atmosphere and the ocean are studied with a simple coupled model. The atmospheric component, based on Lorenz's 1984 model is chaotic and has intrinsic variability at all timescales. The oceanic component models the wind-driven circulation, and has intrinsic variability only in the decadal band. The phase of the cospectrum of atmospheric and oceanic temperatures is examined and it is found that in the decadal band, the oceanic signal leads the atmospheric one, while the opposite is true at shorter and longer timescales. The associated atmosphere-only model, driven by the oceanic temperature derived from a coupled run, synchronizes to the coupled run for arbitrary initial conditions. When noise is introduced in the time series of oceanic driving, episodic synchronization still occurs, but only in summer, indicating that control of the atmosphere by the oceanic variables is prevalent in this season.

1. Introduction

Recent observational (Deser and Timlin 1997) and modeling (Saravanan et al. 2000) studies of the decadal variability in the extratropical ocean–atmosphere system indicate that, despite its large thermal inertia, the ocean is a passive partner. This conclusion is mostly derived from analyzing the time evolution of large-scale spatial patterns of atmospheric and oceanic fields, for example, sea level pressure (SLP) and sea surface temperature (SST). It is typically found that the correlation is maximum when the leading patterns of oceanic variability lag those of atmospheric variability.

There are two paradigms for the ''passive ocean'' driven by an active midlatitude atmosphere. One (Hasselmann 1976) is that sea surface temperature acts as a linear, low-pass filter of the atmospheric temperature signal, which can be treated as a white noise stochastic process. Additional coupling of the atmosphere to the ocean (Bretherton and Battisti 2000) reduces the atmospheric damping at low frequencies reddening the spectrum of atmospheric temperature.

The other paradigm (Palmer 1993) considers the extratropical atmosphere as a low-order, chaotic system, with the oceanic feedback that depends on the recent history of the atmospheric state, without any intrinsic oceanic variability. In this case the ocean provides increased predictability by locking the atmosphere into regimes for longer periods of time.

Both paradigms omit two important elements: first, there is no doubt that the ocean possesses intrinsic variability at interannual and interdecadal timescales, although its effect on the extratropical atmosphere is elusive (Saravanan et al. 2000). Second, the variability in the midlatitude system is strongly modulated by the seasonal cycle. Indeed seasonality is fundamental in the increased predictability of atmospheric patterns from oceanic data. In his early study, Davis (1978) finds a statistically significant correlation between fall and winter SLP anomalies in the North Pacific with anomalies of SST three months earlier, but not in other months. Recent work by Zhang et al. (1998) confirms these results.

In the following, we examine the effects of oceanic variability and seasonality in a simple ocean–atmosphere model. Our strategy for building a conceptual model of the midlatitude coupled system pivots around a low-order chaotic atmosphere that has intrinsic variability at all timescales. In particular, the ultralow frequencies emerge through nonlinear interactions that stem from a single imposed periodicity at the seasonal cycle. This approach is at odds with the notion of a

* Current affiliation: Massachusetts Institute of Technology, Cambridge, Massachusetts.

Corresponding author address: Raffaele Ferrari, Department of Earth, Atmospheric, and Planetary Sciences, Massachusetts Institute of Technology, 77 Massachusetts Ave., Cambridge, MA 02139-4307. E-mail: rferrari@mit.edu

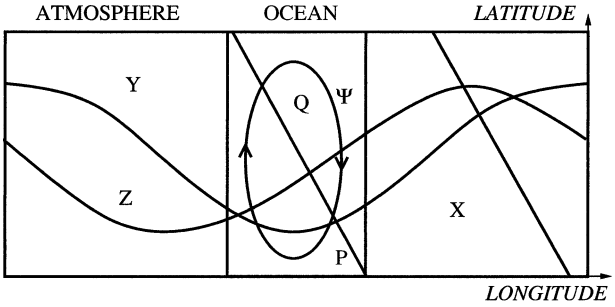

FIG. 1. Schematic of the spatial structure associated with the seven variables that appear in the coupled ocean–atmosphere model described by (4). There are three atmospheric variables: X, the amplitude of the zonally average meridional temperature gradient; Y and Z, the amplitudes of the cosine and sine longitudinal phases of a chain of large-scale waves; and four oceanic variables: P, the zonally averaged meridional temperature gradient at the sea surface; Q, the basin-averaged SST; $\Psi = \psi_r + i\psi_i$, the complex streamfunction that describes the poleward transport of heat by large-scale gyres. The figure illustrates the latitudinal structure associated with X and P and the longitudinal structure associated with Y and Z.

stochastic linear atmosphere in which the spectral amplitudes of different frequency bands are uncorrelated with each other.

The oceanic component has intrinsic time dependence limited to a band centered around a single frequency: this allows us to easily identify the oceanic signature in the coupled system. The atmosphere and the ocean interact by exchanging energy and momentum. We find that although the coupling with the ocean is hard to detect via analysis of the atmospheric time series, it still plays an important role in the evolution of the system.

2. Model formulation

We first describe the separate atmospheric and oceanic models and then introduce the coupling terms.

The atmospheric component is based on the low-order atmospheric general circulation model introduced by Lorenz (1984, 1990). It is defined by these three ordinary differential equations:

$$\begin{aligned} \dot{X} &= -(Y^2 + Z^2) - aX + aF(t), \\ \dot{Y} &= XY - bXZ - Y + G, \\ \dot{Z} &= XZ + bXY - Z. \end{aligned} \tag{1}$$

The independent variable t indicates time, and the overdot indicates a time derivative. The three atmospheric variables are shown in Fig. 1: X represents the amplitude of the zonally averaged meridional temperature gradient (or equivalently, from thermal wind balance, the strength of the zonal mean shear); Y and Z denote the amplitudes of the cosine and sine longitudinal phases of a chain of large-scale waves. Although not shown by Lorenz, these equations can be derived as a Galerkin truncation of the two-layer, quasigeostrophic potential vorticity equations in a channel. In the Lorenz model the poleward heat transport is achieved by the eddies at a rate proportional to $Y^2 + Z^2$, and this heat transport reduces the zonally averaged temperature gradient. The term

$$F(t) = F_0 + F_1 \cos\omega t \tag{2}$$

represents the zonally averaged forcing due to the equator–pole difference in solar heating and it varies on a seasonal timescale ($\omega = 2\pi\ \mathrm{yr}^{-1}$). Here G is a forcing for the longitudinally dependent (nonsymmetric) component representing the sources of east–west temperature differences such as orography and land–sea contrast.

The oceanic module simulates the wind-driven circulation in a basin that occupies a fraction r of the longitudinal extent of the atmosphere (Fig. 1). Its dynamics are described by a set of four ordinary differential equations, namely,

$$\begin{aligned} \dot{P} &= -(\psi_r^2 + \psi_i^2)P, \\ \dot{Q} &= 0, \\ \dot{\psi}_r &= -\sigma\psi_r - \Omega\psi_i, \\ \dot{\psi}_i &= \Omega\psi_r - \sigma\psi_i. \end{aligned} \tag{3}$$

Here P represents the zonally averaged meridional temperature gradient at the sea surface, while Q represents the basin-averaged sea surface temperature. The poleward heat transport is achieved by a large-scale flow, at a rate proportional to $\psi_r^2 + \psi_i^2$ in (3). The average temperature Q is conserved in the absence of any coupling with the atmosphere. The transport is represented by two phases of the streamfunction, ψ_r and ψ_i. The streamfunction undergoes damped oscillations with a period, $2\pi/\Omega$, of 5.3 yr and a decay time, σ^{-1}, of 17 yr. This damped oscillation is the only source of internal variability in the ocean and is due to the intrinsic decadal variability of the wind-driven circulation.

The equations for the two phases of the streamfunction in (3) can be derived as a Galerkin truncation of the one-and-a-half-layer, quasigeostrophic potential vorticity equation for long linear Rossby waves. These long baroclinic waves take the form of basinwide modes of the ocean. Recent work (Cessi and Primeau 2001; LaCasce and Pedlosky 2002) suggests that basin modes with decadal frequencies can be excited by stochastic atmospheric forcing and represent a resonant response of the ocean. This model essentially assumes that the intrinsic decadal variability of the ocean wind-driven circulation is described by one such mode. The quadratic transport law for the zonally averaged temperature P in (3) is derived in several works (Klinger 1996; Wang et al. 1995; Gallego and Cessi 2000). These authors show that for weak flow, the wind-driven gyres reduce the zonally averaged north–south temperature gradient in a basin at a rate proportional to their transport squared. In our model the large-scale ocean gyres are described by the two components of the streamfunction, $\Psi = \psi_r$

TABLE 1. Nondimensional parameters used in the numerical simulations. The dimensional timescale is set to 5 days, so that 1 yr is 73 units long. The nondimensional parameter ξ that appears in the table has the value 8.4×10^{-4}.

a	b	F_0	F_1	G	f	r	c	γ	Ω	σ	α_r	α_i	β_r	β_i
0.025	4	58.5	19.5	1	1	0.23	200	0.55	0.0162	0.000 81	ξ	$\xi/2$	$\xi/2$	$\xi/10$

$+ i\psi_i$, and their squared transport is proportional to $\psi_r^2 + \psi_i^2$.

The feedbacks between the ocean and the atmosphere are constructed so as to conserve total heat in the air–sea exchange. Specifically we set

$$\begin{aligned}
\dot{X} &= -(Y^2 + Z^2) - aX + aF(t) + rf(P - X - \gamma),\\
\dot{Y} &= XY - bXZ - Y + G + rf(Q - Y),\\
\dot{Z} &= XZ + bXY - Z,\\
\dot{P} &= -(\psi_r^2 + \psi_i^2)P + fc^{-1}(X - P + \gamma),\\
\dot{Q} &= fc^{-1}(Y - Q),\\
\dot{\psi}_r &= -\sigma\psi_r - \Omega\psi_i + \alpha_r X + \beta_r Y,\\
\dot{\psi}_i &= \Omega\psi_r - \sigma\psi_i + \alpha_i X + \beta_i Y. \qquad (4)
\end{aligned}$$

The air–sea heat fluxes are proportional to the difference between the oceanic and the atmospheric temperature: these are the terms $f(P - X)$ and $f(Q - Y)$ (Haney 1971). The bulk transfer coefficient, f, is assumed to be constant. In the atmospheric model this term needs to be multiplied by the fraction of earth covered by ocean, r. In the oceanic model the air–sea flux is divided by c, which is the ratio of the vertically integrated heat capacities of the atmosphere and the ocean. The constant γ represents the fraction of solar radiation that is absorbed directly by the ocean. There is no heat exchange between the atmospheric standing wave Z and the ocean, because Z represents the sine phase of the longitudinal eddies and has zero zonal mean across the ocean (Fig. 1). A feedback between Z and the ocean would appear if we added an equation for the longitudinal temperature gradient of the ocean.

The effect of the wind stress acting on the ocean is represented as a linear forcing proportional to X and Y in the equations for the streamfunction, ψ. The coupling constants α_r, α_i, β_r, and β_i are chosen to produce realistic values for the oceanic heat transport.

Different experiments showed that the results presented in the rest of paper are quite robust to changes in the parameters that appear in (4) as long as the model remains chaotic, as explained in the following section. However the variables retain realistic values only for a limited range of the external parameters. This consideration dictated the particular set given in Table 1, which is used throughout the paper.

3. Results

The uncoupled Lorenz model in (1) admits several regimes depending on the parameters, including a chaotic regime and an intransitive regime. The latter is characterized by one of two possible periodic solutions, each selected by the initial conditions. The amplitude of the forcing, F, is one of the parameters controlling which dynamical regime is achieved. When the forcing is time dependent, as in (2), a judicious choice of the parameters leads to an unpredictable alternation of the two periodic regimes during the summer months, while the winters are chaotic. Because the onset of any of these regimes is unpredictable, the atmospheric system has interannual variations. The ultralow frequency thus obtained leads to a spectrum that is flat for periods longer than one year. However, because of the strong locking to the seasonal cycle the phases of the atmospheric signal are not random as those of a stochastic process. The point here is that the atmospheric spectrum is close to that of a white noise signal, as suggested by Hasselmann (1976), but the atmospheric dynamics are not stochastic. In other words, spectra, by themselves, do not adequately describe atmospheric variability.

The atmospheric temperature gradient, X, displays the same behavior in the coupled model, as shown in Fig. 2 (top): some summers have small amplitude oscillations while others are locked into a weak temperature gradient. Winters exhibit larger variability and are chaotic. A comparison with the atmosphere-only model (1) for the same parameter values shows that the residence time in the quiet summer regime is longer in the coupled system, while the winter's variability is comparable to that obtained in the atmosphere-only calculations (Palmer 1993). It appears as if the coupling with the ocean has little effect on the atmosphere. However, we will demonstrate that this is not the case.

The coupled dynamics

Before describing the variability of the coupled model, it is worth mentioning that for the choice of parameters in Table 1, the time-averaged variables have values consistent with observations of the present climate. In particular, we find that the ratio of the atmospheric to the oceanic heat transport is given by

$$\upsilon T_{\rm atm}/\upsilon T_{\rm ocn} = \overline{(Y^2 + Z^2)}/\overline{rc(\psi_r^2 + \psi_i^2)P} \approx 8.5, \qquad (5)$$

in rough agreement with the estimates for the midlatitude North Atlantic recently summarized by Trenberth and Caron (2001). Similarly, the ratio of atmospheric to oceanic mean temperature gradient is given by

$$T_{\rm atm}/T_{\rm ocn} = \overline{X}/\overline{P} \approx 1.8. \qquad (6)$$

Other aspects of this low-order model are less real-

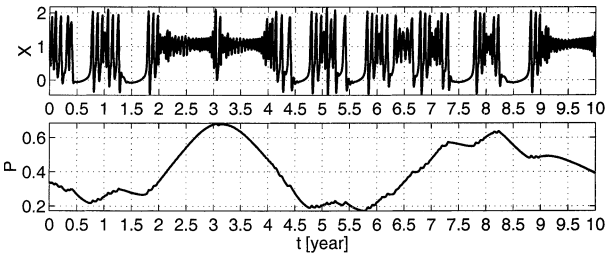

FIG. 2. Time series of the of (top) atmospheric, X, and (bottom) oceanic, P, temperature gradients from a 50-yr run of the coupled model in (4) with the parameters given in Table 1. Six ''quiet summers'' (years 0.5, 1.5, 4.5, 5.5, 7.5, and 8.5) are noted in the atmospheric series.

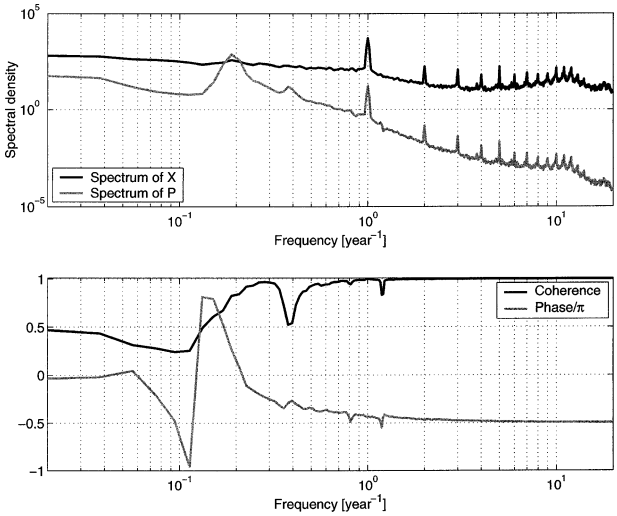

FIG. 3. Spectral estimates of typical simulations (40 realizations each 53 yr long): (top) the spectrum of the atmospheric temperature gradient X (black) has peaks at the seasonal cycle and its superharmonics, while the spectrum of the oceanic temperature gradient P (gray) has an additional peak centered at $\Omega/2\pi = 0.19$ yr^{-1}; (bottom) the coherence of X and P (black) is close to unity for periods shorter than five years, and the phase (gray) is negative indicating that the ocean, P, lags the atmosphere, X. In the decadal band the coherence is somewhat smaller, though still significant, and the phase is positive, implying that P leads X.

istic; for example, two clear regimes exist in summer, while in the present atmosphere four regimes are identified and they are most evident in winter (Corti et al. 1999). However, the formulation in (4) captures the qualitative notion that the climate attractor has a multimodal probability density function, and atmospheric low-frequency variability largely arises from transitions among these regimes.

Because the model ocean is driven by the atmosphere, oceanic variability is a low-pass-filtered image of the atmospheric variability, except at the period of 5.3 yr. This is illustrated in Fig. 2, which shows a portion of the time series of the atmospheric and oceanic variables for a calculation with the parameters set to the values in Table 1.

Spectra of atmospheric, X, and oceanic, P, temperature gradients are shown in Fig. 3 (top). Both spectra are dominated by the seasonal cycle and its harmonics, and the ocean also exhibits a peak at its intrinsic frequency (1/5.3 yr^{-1}).

We also calculated the cospectrum of X and P (Bendat and Piersol 1986); at almost all frequencies the coherence is close to unity and the corresponding phase is negative implying that the ocean follows the atmosphere (Fig. 3, bottom). At periods longer than about 5 yr, the coherence drops, but is still high for periods less than 10 yr: in the band with periods between 5 and 10 yr the phase is positive indicating that *the ocean leads the atmosphere*.

Linear thinking would suggest that an atmosphere lagging an oscillating ocean should exhibit a spectral peak at the oceanic frequency. However, there is no evidence of the oceanic intrinsic frequency in the atmospheric spectrum (Fig. 3, top). But absence of evidence is not evidence of absence: the ocean is not passive, as demonstrated by the phase of the cospectrum. The oceanic role is not apparent because at these low frequencies the atmosphere has a broadband intrinsic variability that masks the oceanic contribution.

Our results show that the phase of the cospectrum is a robust diagnostic for uncovering the relationship between signals in a given frequency band. Other diagnostics, such as the correlation, average the cospectrum over many frequencies so that any lead by the ocean in specific frequency bands is masked by the atmospheric lead at other frequencies.

Notice that despite the complexity of the atmospheric temperature gradient time series (Fig. 2, top), and the broadness of its low-frequency spectrum (Fig. 3, top), the dynamics are chaotic, and not stochastic. This implies a strong phase correlation between the atmosphere and the ocean *at all timescales*. To illustrate this connection an atmosphere-only model is used, driven by the oceanic variables $P_c(t)$ and $Q_c(t)$ obtained from a separate coupled run with the same parameters and a different initial condition. That is, we integrate (4) with prescribed $P_c(t)$ and $Q_c(t)$. This is typically referred to as a driven system.

Figure 4a shows the time series of the difference in the atmospheric temperature gradients obtained with the coupled model, $X_c(t)$, and with the prescribed ocean-temperature model, $X_u(t)$: after about 15 years the uncoupled time series synchronizes to the coupled time series (Fig. 4a). The synchronization occurs for every initial condition, although the time of synchronization depends on the initial state. This is an example of synchronized chaos (Strogatz 1994): regardless of the initial state of the atmosphere, when the atmosphere is *driven by* (rather than *coupled to*) the oceanic variables, $P_c(t)$ and $Q_c(t)$, the resulting system is no longer chaotic.

This is a striking demonstration that, at least in this model, although ocean variability has no expression in atmospheric spectra its dynamics are essential to the

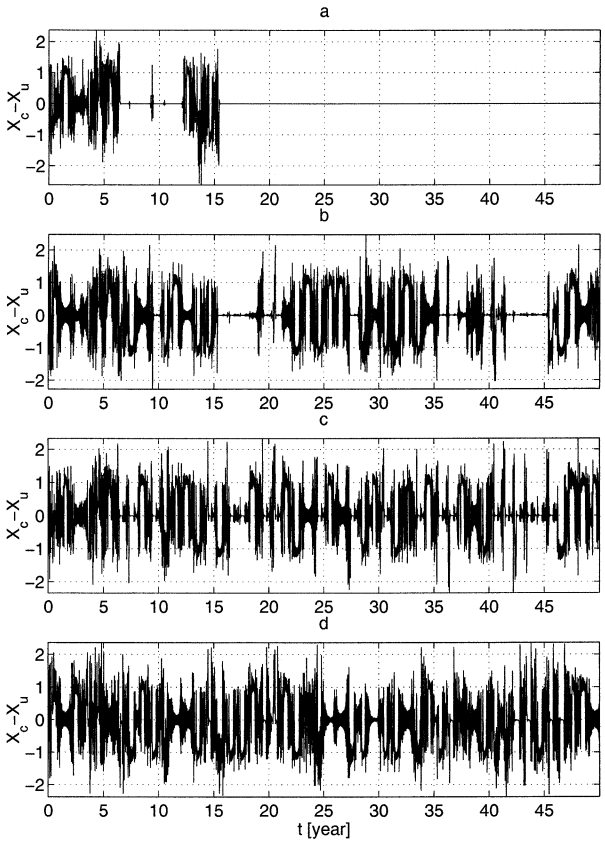

FIG. 4. Synchronization. (a) Difference between the atmospheric gradient, X_c, obtained by running a coupled simulation with an active ocean and X_u, obtained by running a simulation with the ocean variables, P_c and Q_c, given by the coupled run. The two runs differ in the initial condition of the atmosphere. (b) Difference between X_c and X_u, where X_u is now obtained by running a simulation with the ocean temperature given by the coupled run plus a noise with $\epsilon = 10^{-3}$. (c), (d) Same as (b) but with noises of amplitude $\epsilon = 10^{-2}$ and $\epsilon = 10^{-1}$, respectively.

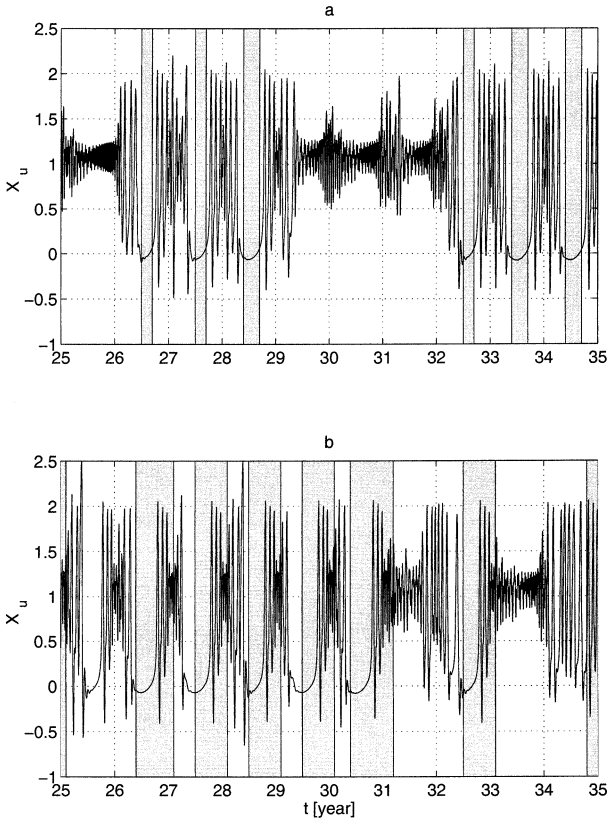

FIG. 5. A subsection of the uncoupled atmospheric temperature gradient X_u for two runs with the oceanic variables, P_c and Q_c corrupted with noise of amplitude (a) $\epsilon = 10^{-1}$ and (b) $\epsilon = 10^{-2}$. The gray patches highlight periods during which X_u is synchronized with the coupled run, X_c; that is, time intervals of at least 30 days in which $|X_u - X_c| < 10^{-2}$. Notice that synchronization is seasonal and only occurs during ''quiet'' summers, i.e., summers where the atmospheric gradient is weak and slowly varying.

behavior of the atmospheric component. For our choice of parameters both the coupled ocean–atmosphere system, (4), and the atmosphere-only system, (1), are chaotic, but the driven ocean-temperature model is not. That is, the prescribed ocean puts the atmosphere on a specific trajectory in phase space and eliminates the sensitive dependence on initial conditions. Indeed, it can be shown (Pecora and Carroll 1990) that all the Lyapunov exponents of the driven system are negative. This raises questions of what we mean by a passive ocean. Our ocean has no visible effect on the atmospheric spectrum and lags the atmosphere at nearly all frequencies. However the ocean clearly plays a major part in the coupled evolution of the system. Prescribing the ocean variables eliminates the unpredictable behavior of the atmosphere.

Recovery of the ''true solution'' is only achieved if the oceanic time series used in the uncoupled model are ''perfect.'' Adding noise to the prescribed ocean temperature model inhibits a permanent synchronization to the coupled time series. However even with an ''imperfect'' knowledge of the ocean, the ''true'' atmosphere is recovered over finite intervals of time, and we obtain ''episodic synchronization.'' Figures 4b,c,d show $X_c - X_u$ for 50-yr runs in which the atmosphere is forced by the prescribed ocean temperature from the coupled model, P_c and Q_c, corrupted with white noise. That is at every time step, we add to P_c and Q_c a random variable sampled uniformly between $\pm\epsilon$. Figures 4b,c,d are examples with ϵ equal to 10^{-3}, 10^{-2}, and 10^{-1}, respectively. These amplitudes correspond to rms errors in P_c and Q_c of 0.05%, 0.5%, and 5%, respectively.

As illustrated in Fig. 5, synchronization is established at the beginning of summers characterized by a weak temperature gradient, because in these quiet and persistent summers the atmosphere displays a quasiperiodic behavior that is easily driven by the oceanic temperature. Indeed, the coupled system during these periods shows no evidence of chaotic behavior and this portion of the attractor is not sensitive to small differences in the initial conditions.

There are, however, stretches of many years in which

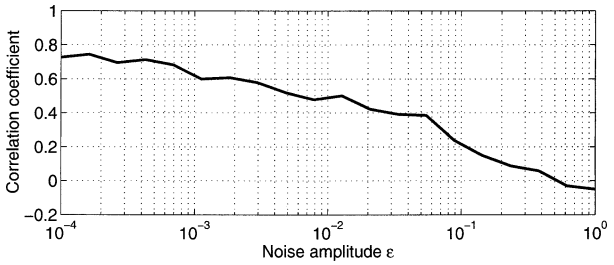

FIG. 6. Correlation coefficient as a function of the noise amplitude ϵ between X_c obtained by running a coupled simulation with an active ocean and X_u obtained by running a simulation with the ocean temperature given by the coupled run. Because of the initial transient, the correlation does not approach unity as $\epsilon \to 0$ for time series of finite length.

synchronization is not observed. This is because synchronization can only occur in summer, never during the chaotic winters, and the asynchronous years have summers that fall on a different periodic orbit, characterized by rapid oscillations. For large noise, synchronization is lost by the beginning of the following winter, while as the noise decreases it persists through winters and sometimes for multiple years.

The driven runs in which the oceanic temperature is prescribed can be considered as a reanalysis in which oceanic observations are assimilated in the atmospheric model. The onset of synchronization in summer suggests that control of the atmosphere from the ocean is higher in this season. The time series of oceanic temperature drives the atmosphere on the attractor during quiet summers and provides the correct initial conditions for the coupled run. During chaotic winters synchronization is unlikely to be initiated. This scenario is different from that of a linear ocean coupled to a stochastic atmosphere. In that case the ocean acts as a low-pass filter of the atmospheric variables. Assimilating such an ocean into the coupled model could recover only the low-frequency variability of the atmosphere.

In chaotic models, a long enough time series of even one single variable contains enough information to reconstruct the whole system. This is because the deterministic dynamics locks the phases of different variables at all frequencies. Thus, although the phase of the cospectrum in Fig. 3 suggests a role of the ocean limited to long periods, all timescales are important. Our noisy synchronization results indicate that the behavior of the coupled system can be recovered most efficiently during certain times of the year, that is, in the quiet summers.

The seasonality of synchronization is consistent with the behavior observed by Davis (1978) in the analysis of SST and SLP anomalies in the North Pacific. Fall and winter SLP tends to be well predicted by summer SST. Similarly, in our system synchronization is established in the summer and lasts for a few months in the fall (Fig. 5b).

The correlation coefficient between X_c and X_u is a good indicator of how robust synchronization is to the addition of noise (Fig. 6). As the noise added to the oceanic variables grows, the correlation coefficient decreases from a value of 1, indicating that the model spends less and less time in the synchronized state.

4. Conclusions

We take the point of view that midlatitude atmospheric variability is generated by nonlinear interactions between baroclinic eddies and the mean zonal flow leading to chaotic motions. The variability is strongly modulated by the seasonal cycle. These dynamics alone provides a spectrum that is white at timescales longer than one year, but whose phases are not random as those of a stochastic process. A conceptual atmospheric model that fulfills these criteria is Lorenz (1984, 1990) and we study the effect of coupling this model to an ocean model.

Although the atmosphere has interannual and interdecadal intrinsic variability, we find that an ocean with intrinsic decadal oscillations leads the atmospheric fluctuations at these timescales when the two systems are coupled. The phase relation between the atmosphere and the ocean is best revealed by examining the cospectrum of the two signals.

By examining the associated system where an atmosphere-only model is driven by the oceanic variables obtained from a coupled run, we establish that the leading role of the ocean is due to phase locking of the atmospheric to the oceanic signal during summers characterized by a persistent state. During these seasons the atmosphere has a weak temperature gradient, the baroclinic activity is reduced, and there is no chaotic variability. Then, prescription of the oceanic temperature into an atmosphere-only model leads to phase locking. The phase locking becomes permanent if the driving oceanic variables are known perfectly. If the driving oceanic variables are degraded by noise, the atmospheric signals from the driven and coupled systems synchronize episodically during these quiet summer months. Furthermore, because the atmospheric Lorenz model (1) without an ocean has fewer and less persistent quiet summers for the same values of parameters, we speculate that coupling to the ocean leads to increased predictability and that this effect is achieved during these quiet summers. The stabilizing role of the ocean in the midlatitude atmosphere has also been remarked upon by Palmer (1993). Our model further indicates that the stabilizing effect of the midlatitude atmosphere by the ocean is prevalent in summer. Seasonal dependence is also found in El Niño predictions, although it is not clear whether it arises from the extrinsic seasonal modulation or from the intrinsic timing of the perturbations' amplification (Samelson and Tziperman 2001).

This model suggests that in midlatitudes the feedbacks between the ocean and the atmosphere are difficult to detect, because the atmospheric variability is dominated at all frequencies by forcing at the seasonal cycle.

However there are strong correlations between the phases of the two systems, especially in the summer season, as supported by Davis's (1978) analysis of North Pacific data. The observational challenge is to find appropriate statistics that extract these seasonal phase relations. The situation is different in the Tropics, where the seasonal modulation is weaker. As a result coupled patterns, like El Niño, are apparent in the time series of the atmospheric and oceanic patterns and not only in the phase correlations between the two systems.

Acknowledgments. This work was conducted at the 2001 WHOI GFD Summer Program, which is supported by the National Science Foundation and the Office of Naval Research. We thank the director, Neil Balmforth, for organizing the program. Additional support was provided by the Woods Hole Postdoctoral Fellowship (Ferrari) and by the Department of Energy (Cessi). We benefited from comments and suggestions by two anonymous reviewers.

REFERENCES

Bendat, J. S., and A. G. Piersol, 1986: *Random Data: Analysis and Measurement Procedures.* 2d ed. Wiley-Interscience, 566 pp.

Bretherton, C. S., and D. S. Battisti, 2000: An interpretation of the results from atmospheric general circulation models forced by the time history of the observed sea surface temperature distribution. *Geophys. Res. Lett.,* **27,** 767–770.

Cessi, P., and F. Primeau, 2001: Dissipative selection of low-frequency modes in a reduced-gravity basin. *J. Phys. Oceanogr.,* **31,** 127–137.

Corti, S., F. Molteni, and T. N. Palmer, 1999: Signature of recent climate change in frequencies of natural atmospheric circulation regimes. *Nature,* **398,** 799–802.

Davis, R. E., 1978: Predictability of sea level pressure anomalies over the North Pacific Ocean. *J. Phys. Oceanogr.,* **8,** 233–246.

Deser, C., and M. S. Timlin, 1997: Atmosphere–ocean interactions on weekly timescales in the North Atlantic and Pacific. *J. Climate,* **10,** 393–408.

Gallego, B., and P. Cessi, 2000: Exchange of heat and momentum between the atmosphere and the ocean: A minimal model of decadal oscillations. *Climate Dyn.,* **16,** 479–489.

Haney, R. L., 1971: Surface thermal boundary conditions for ocean circulation models. *J. Phys. Oceanogr.,* **1,** 241–248.

Hasselmann, K., 1976: Stochastic climate models. Part I: Theory. *Tellus,* **28,** 473–485.

Klinger, B. A., 1996: A kinematic model of wind-driven meridional heat transport. *J. Phys. Oceanogr.,* **26,** 131–135.

LaCasce, J. H., and J. Pedlosky, 2002: Baroclinic Rossby waves in irregular basins. *J. Phys. Oceanogr.,* **32,** 2828–2847.

Lorenz, E. N., 1984: Irregularity: A fundamental property of the atmosphere. *Tellus,* **36A,** 98–110.

——, 1990: Can chaos and intransitivity lead to interannual variability? *Tellus,* **42A,** 378–389.

Palmer, T. N., 1993: Extended-range atmospheric prediction and the Lorenz model. *Bull. Amer. Meteor. Soc.,* **74,** 49–65.

Pecora, L. M., and T. L. Carroll, 1990: Synchronization in chaotic systems. *Phys. Rev. Lett.,* **64,** 821–824.

Samelson, R. M., and E. Tziperman, 2001: Instability of the chaotic ENSO: The growth-phase predictability barrier. *J. Atmos. Sci.,* **58,** 3613–3625.

Saravanan, R., G. Danabasoglu, S. C. Donney, and J. C. McWilliams, 2000: Decadal variability and predictability in the midlatitude ocean–atmosphere system. *J. Climate,* **13,** 1073–1097.

Strogatz, S. H., 1994: *Nonlinear Dynamics and Chaos.* Addison-Wesley, 498 pp.

Trenberth, K. E., and J. M. Caron, 2001: Estimates of meridional atmosphere and ocean heat transports. *J. Climate,* **14,** 3433–3443.

Wang, X., P. H. Stone, and J. Marotzke, 1995: Poleward heat transport in a barotropic ocean model. *J. Phys. Oceanogr.,* **25,** 256–265.

Zhang, Y., J. R. Norris, and J. M. Wallace, 1998: Seasonality of large-scale atmosphere–ocean interaction over the North Pacific. *J. Climate,* **11,** 2473–2481.